

Semi-Analytical Minimum Time Solutions with Velocity Constraints for Trajectory Following of Vehicles [★]

Marco Frego^b, Enrico Bertolazzi^a, Francesco Biral^a, Daniele Fontanelli^a,
Luigi Palopoli^b

^a*DII - Dipartimento di Ingegneria Industriale - University of Trento - Trento, Italy*

^b*DISI - Dipartimento di Ingegneria e Scienza dell'Informazione - University of Trento - Trento, Italy*

Abstract

We consider the problem of finding an optimal manoeuvre that moves a car-like vehicle between two configurations in minimum time. We propose a two phase algorithm in which a path that joins the two points is first found by solving a geometric optimisation problem, and then the optimal manoeuvre is identified considering the system dynamics and its constraints. We make the assumption that the path is composed of a sequence of clothoids. This choice is justified by theoretical arguments, practical examples and by the existence of very efficient geometric algorithms for the computation of a path of this kind. The focus of the paper is on the computation of the optimal manoeuvre, for which we show a semi-analytical solution that can be produced in a few milliseconds on an embedded platform for a path made of one hundred of segments. Our method is considerably faster than approaches based on pure numerical solutions, it is capable to detect when the optimal solution exits and in, this case, compute the optimal it. Finally, the method explicitly considers non-linear dynamics, aerodynamic drag effect and bounds on the longitudinal and on the lateral acceleration.

Key words: Autonomous vehicles; Optimal control; Trajectory planning; Efficient algorithms; Time-optimal control; Nonlinear systems; Path planning; Riccati differential equations; Splines; Velocity saturation

1 Introduction

Over the past twenty years, the polar star for a large number of research activities has been how to introduce artificial intelligence into automobiles in order to make them safer, environment friendly and autonomous. The main actors of this impressive and consistent effort have been top academic institutions, research funding agencies such as DARPA and the European Commission, automotive industries and, more recently, important players in the Information and Communication Technologies area such as Google and Apple. Some tangible results of this activity are already available in modern commercial cars in the form of technological packages

for lane keeping, autonomous braking, pedestrian detection and active cruise control. The next stride will likely push a new generation of cars straight into the realm of autonomous driving. This is far from being a remote possibility: starting from 2015 Tesla cars allow the user to switch to autopilot mode, although under her/his legal responsibility for possible accidents [21]. Successful examples of cars driving autonomously for thousand of miles have been documented in the scientific literature [12,23], but some crucial research problems are still there in search of cost effective and robust solutions. One of these is planning trajectories for vehicles manoeuvring at high speed, pushed to their dynamic limit and in presence of moving or fixed obstacles. Trajectory planning in such extreme driving scenarios requires robust computational methods to produce a number of alternative feasible manoeuvres to choose from in a small time.

[★] This work was partially supported by the Autonomous Province of Trento project “OptHySYS - Optimal Hybrid Systems”.

Email addresses: marco.frego@unitn.it (Marco Frego), enrico.bertolazzi@unitn.it (Enrico Bertolazzi), francesco.biral@unitn.it (Francesco Biral), daniele.fontanelli@unitn.it (Daniele Fontanelli), palopoli@disi.unitn.it (Luigi Palopoli).

Related Work. When the vehicle speed is high and the driving conditions extreme, the application of a purely geometric approach such as optimal geometric

path planning [18] falls short of the expectations and the dynamic constraints have to be put in their proper place [40]. In this context path planning solutions based on optimal control hold the promise to produce high quality manoeuvres that account for the vehicle dynamics and for the related constraints and can realistically be tracked by a vehicle [4,9,32,36,43]. The price to pay is the high computational cost incurred and the absence of any guarantee on the generation of feasible solutions. Both problems make such algorithms hardly a viable choice for real-time (reactive) planning or for the production of a large number of potential trajectories in a small time.

This consideration has motivated several authors to seek different solutions. One possible method is based on the fast generation of feasible kinematic trajectories *via* direct search and on the subsequent refinement of the solution by incorporating dynamic properties [15,31,44]. Such approaches have the considerable advantage to always produce feasible solutions, albeit not generally optimal. An interesting and new research area uses differential flatness to transform the problem from the canonical state space to flat output variables, where the solution is independent from the differential model equations [33,38]. Flat methods require to approximate the optimal function on a polynomial basis and solve the associated NLP to optimise the target function (e.g. minimum time in our case). It is known from [13] that bang-bang problems are not particularly suitable for this method because of the intrinsic discontinuous nature of the solution, unless continuity is enforced. However, the main drawback of those solutions is that it is not possible to avoid purely numeric computations to deal with constraints, that are computationally slower than analytic or semi-analytic solutions. A possible alternative to produce near-optimal solutions in a small amount of time with a guaranteed convergence is by a hierarchical approach. A *master* optimisation problem generates several alternative paths, reasoning at a geometric level, while a *slave* optimisation generates the optimal manoeuvres for each of the considered paths accounting for the dynamics of the vehicle and for the constraints. Based on the results of the slave, the master selects the path for which the generated trajectory has the best performance. By decoupling geometric from dynamic planning, it is possible to consider a variety of different constraints for each of the two (e.g., presence of obstacles in the geometric part or acceleration constraints in the dynamic part) putting in place the most appropriate solutions. On the contrary a monolithic formulation encompassing both the geometric and the dynamic part can potentially give rise to serious complexity and scalability issues. The available options for an effective design of a master algorithm are quite a few and range from stochastic sampling algorithms such as RRT/RRT* [28,29,30] to particle swarming [37], from graph based approaches [39] to potential fields [3]. Whatever the choice of the master algorithm (a first example implementing this idea of master/slave problem

decomposition using RRT* can be found in [20]), the large number of times the slave problem has to be solved makes its efficiency key to the viability of the whole idea. In this work, we propose a solution for a *minimum time manoeuvre over a given sequence of clothoid curves* for a car-like vehicle subject to acceleration constraints. This is a close suboptimal solution for a more general trajectory planning problem: moving a car-like vehicle in minimum time between two configurations. The convenience of choosing clothoids as basic motion primitive derives from a few observations. One reasonable and widely adopted assumption is that the driver actuates the steering wheel without discontinuities, making the curvature of the path a continuous function (see, for instance, Fraichard et al. [18]). By choosing the simplest continuous curvature function (i.e., a piecewise linear function) the resulting path is a sequence of clothoids. The case of zero curvature (i.e., straight lines), and the case of constant curvature, (i.e., arc of circle) are special cases of a clothoid. Such curves are known to be the fundamental building block for minimum time manoeuvres for the Dubins car [16], i.e., a unicycle that moves at constant speed. Moreover, for an actual car vehicle having the velocity modelled as a linear ODE, it can be shown that the limitations of the lateral velocity produce exactly a clothoid. Finally, producing a clothoid that joins two points optimising some geometric cost is a problem for which efficient solutions exist [5]. Other methods to produce a geometric path include fast generators of Kappa [1] and Gamma [25] trajectories, which are made of sequences of straight segments and circular arcs. The discontinuous curvature thus obtained is more suitable for holonomic vehicles than for car vehicles. It has to be noted that our algorithm is capable to find the optimal speed profile for those kind of paths too, since segments and circular arcs are particular cases of clothoids.

Paper Contributions. In the paper, we will offer additional arguments and numeric examples to support our choice of using clothoids. Then, we will propose a *semi-analytical* solution to find the optimal manoeuvre for a single clothoid is based on a direct application of the Pontryagin Maximum Principle. An important feature of our work is the explicit consideration of quadratic drag term in the longitudinal dynamics of the vehicle. This term is mandatory for the proper description of high speed manoeuvres and is usually managed *via* numeric integration. In our setting, the consideration of the term does not disrupt the analytical form of the solution, which is made of segments where the acceleration has to be maximum or minimum and segments in which it is given by a simple analytic expression. The switching points between the different segments are found *via* the solution of simple polynomial equations. The application of semi-analytical solutions for optimal control problems in the context of motion planning has been championed by [24,45], who studied the minimum time control strategy that accounts for the vehicle dynamics,

speed and control constraints over a given trajectory. The authors resort to numeric solutions for forward and backward integration. With respect to this work, our analytic condition considers complex non-linear dynamics and constraints (e.g., aerodynamic drag) and does not rely on any type of forward and backward numeric integration. In a different context Da Lio et al. [14] propose semi-analytical solutions to represent the motor primitives at the basis of the complex manoeuvres generated by a human driver. However, the model they use does not consider acceleration and speed constraints and the cost function that they optimise is related to weighted minimisation of jerk and time without any constraints on states and controls whereas we consider a constrained pure minimum time problem. Another important contribution of our paper is an algorithm to construct the optimal solution for a sequence of clothoid segments starting from one, and a theorem stating the optimality of the result.

The efficiency of our solution makes us confident that our work can be credibly used as building block for the slave algorithm in the hierarchical scheme outlined above. Although the main motivations of the paper are rooted in the automotive domain, we expect a full applicability of our results in a variety of different applications (e.g., guidance of AGVs in industrial applications). Furthermore, our solution allows us to consider the manoeuvrability envelope (ME) of the vehicle in terms of g-g diagram [8,34]. The ME characterises all feasible manoeuvres and it condenses information on maximum achievable performance and on state reachability as well as human driving preferences [11]. This paper subsumes the preliminary results reported in [19] and extends those findings in these respects: 1. A deep analysis and a numerical proof of the validity of the adopted car-like model is now reported; 2. The optimal control problem has been extended from a single to an arbitrary number of clothoids (i.e., a sequence). This extension is non trivial because of the discontinuity in the optimal control as well as the presence of constraints on the maximum lateral acceleration, which makes the problem non purely bang-bang; 3. Finally, the overall algorithm for the time optimal control synthesis for a path of an arbitrary length has been defined and its optimality provided. Moreover, it has been tested on an embedded platform experimentally showing its higher performance with respect to state of the art solutions.

The paper is organised as follows. Section 2 gives a general formulation of the problem discussing models and constraints. In the same section, we also produce theoretical arguments and numeric examples for our choice of clothoid arcs as a basic primitive for geometric planning, and reformulate the problem in this setting using curvilinear coordinates. Section 3 presents the semi-analytical solution for the case of a single clothoid, and Section 4 generalises to the case of a path composed of a sequence of clothoid arcs. Section 5 shows some numeric examples proving the efficiency of our solution. Finally, Section 6

draws the conclusions of the paper and announces future work directions.

2 Problem Description

This paper is about finding time-optimal trajectories for a car-like vehicle under acceleration constraints. In general terms, the problem can be formulated as follows.

Problem 1 Find controls $\mathbf{u}(t)$ in a compact set that minimises the total time T subject to:

$$\text{ODE: } \dot{\mathbf{x}}(t) = \mathbf{f}(\mathbf{x}(t), \mathbf{u}(t)),$$

$$\text{Boundary Conditions: } \mathbf{x}(0) = \mathbf{x}_0, \mathbf{x}(T) = \mathbf{x}_f,$$

$$\text{Constraints: } \mathbf{h}(\mathbf{x}(t)) \leq \mathbf{0},$$

where $\mathbf{x}(t)$ are the state variables describing the position and velocity of the vehicle along the trajectory and $\mathbf{u}(t)$ are the control variables.

The control variables are the steering turning radius $\bar{\delta}(t)$ and the longitudinal acceleration $a(t)$. The dynamics of the vehicle are described by the smooth function $\mathbf{f}(\cdot, \cdot)$. The function $\mathbf{h}(\cdot)$ collects all the constraints on longitudinal and lateral acceleration, which emanate from the physical limitations of the actuators (brakes or engine) and from the adherence limit between the tyre and the ground. In the next subsection, we will introduce realistic models and constraints to populate the optimisation problem above with explicit expressions for $\mathbf{f}(\cdot, \cdot)$ and $\mathbf{h}(\cdot)$.

Our strategy to solve Problem 1 is to produce a close approximation of the optimal solution by *constraining the vehicle to move along a sequence of clothoids*. To this purpose, we will discuss a reformulation of the car-like model for the motion along an assigned clothoid providing theoretical and practical arguments for this choice. This simplification is possible after a deep analysis of models and constraints, exposing important non-linear effects in the longitudinal dynamics. The rest of this section is devoted to this discussion.

2.1 Modelling

In order to develop analytic techniques for the problem of path generation the kinematic model used has to strike a good compromise between realism and tractability. A good starting point can be the car-like kinematic model, which in xy -coordinates is given by:

$$\begin{bmatrix} \dot{x} \\ \dot{y} \\ \dot{\psi} \\ \dot{\delta} \end{bmatrix} = \begin{bmatrix} \cos \psi \\ \sin \psi \\ \tan \delta / l \\ 0 \end{bmatrix} v + \begin{bmatrix} 0 \\ 0 \\ 0 \\ 1 \end{bmatrix} \bar{\omega}, \quad (1)$$

where ψ is the orientation (yaw angle) of the vehicle with respect to a right-handed reference frame having the Z axis perpendicular to the (X, Y) plane of motion, δ is the steering angle, v is the forward velocity of the vehicle, $\bar{\omega}$ is the normalised angular velocity of the steering wheel and $l > 0$ is the wheelbase. When this model is used with a constant velocity v , the optimal minimum time solution is given by a sequence of clothoids. This property, recognised by Fraichard et al. [18], is not true in the general case (i.e., changing velocity), for which the time optimal solution has a curvature depending on the nonlinear ODE linking $\dot{\delta}$ with the velocity profile v . However, our experience with concrete case-studies (reported in part in Section 5) reveals that also with a varying velocity v , the curvature of the path for the model (1) is very close to a piecewise linear function, which is the defining property of a clothoid. A formal explanation of this fact is offered next. By making the change of variable $\delta = \tan \delta$ and by introducing the virtual control ω we obtain the following model:

$$\begin{bmatrix} \dot{x} \\ \dot{y} \\ \dot{\psi} \\ \dot{\delta} \end{bmatrix} = \begin{bmatrix} \cos \psi \\ \sin \psi \\ \delta/l \\ 0 \end{bmatrix} v + \begin{bmatrix} 0 \\ 0 \\ 0 \\ 1 \end{bmatrix} \omega, \quad \omega = (\delta^2 + 1) \bar{\omega}. \quad (2)$$

In this new state space, the minimum time trajectory is composed exactly by a sequence of clothoids. To see this, simply transform the independent variable t to the curvilinear abscissa s , e.g., divide the r.h.s. of (2) by v . The resulting equations, where the control appears linearly, lead to an optimal bang-bang controller generating a clothoid. As far as $\tan \delta$ can be approximated to δ (which is typically the case for automotive systems), the deformation introduced by the change of variable is moderate. Potentially more troublesome is the introduction of the auxiliary control ω in (2), which in fact restricts the space of admissible control functions leading to a suboptimal solution. Our results reveal that the impact of this restriction is not very large in the face of the radical simplification introduced in the solution of the optimisation problem.

2.1.1 Longitudinal Dynamics

The evolution of the longitudinal velocity $v(t) \geq 0$ is in general coupled with the lateral dynamics. The 2D equations of motion of a front steering double track vehicle under the reasonable assumption of small steering angle (see [22], Ch. 3) are

$$\begin{aligned} m(v' - \Omega v \beta) &= \sum_{i=1}^4 F_x^i(a_y, a_x, \delta) - \sum_{i=1}^2 \delta F_y^i(a_x, a_y, \delta) \\ &\quad - c_r mg - k_{v0} v - k_{v1} v^2, \\ m((\beta v)' + \Omega v) &= \sum_{i=1}^4 F_y^i(a_x, a_y, \delta) + \sum_{i=1}^2 \delta F_x^i(a_x, a_y, \delta) \end{aligned}$$

where, c_r is the rolling friction coefficient, k_{v0} linearly velocity dependent friction coefficient, k_{v1} is the aerodynamic drag coefficient, m is the vehicle total mass, $\Omega = \psi'$ is the yaw rate, β is the body slip angle that is the angle between the absolute velocity of the centre of mass V and the symmetrical axis of the vehicle (as shown in Figure 4). $F_x^i(\cdot)$ and $F_y^i(\cdot)$ represent respectively the longitudinal and lateral force contributions of each tyre and $i = 1, 2$ indicating the front left and right tyres and $i = 3, 4$ the rear left and right tyres where are respectively the longitudinal and lateral acceleration of the vehicle centre of mass. Those forces are in general quite nonlinear and function of longitudinal and lateral accelerations of centre of mass (i.e. a_x, a_y) and the steering angle δ . Under the hypothesis above that $\beta \approx 0$ (i.e. vehicle tangent to the trajectory) we can assume that $(\beta v)' \approx 0$ and $\Omega \beta v \approx 0$ and therefore the longitudinal acceleration becomes $a_x \approx v'$ and the lateral acceleration $a_y \approx \Omega v$. The second equation, which governs the lateral dynamics, reduces to an algebraic one that can be solved for the lateral force necessary to keep the vehicle on the trajectory as function of lateral acceleration a_y . Thus calling $F_x = \sum_{i=1}^4 F_x^i(a_y, a_x, \delta)$ the total force in the longitudinal direction, the equation of the longitudinal dynamics reduces to :

$$mv' = F_x - \sum_{i=1}^2 \delta F_y^i(a_x, a_y, \delta) - c_r mg - k_{v0} v^2$$

Normalising with the mass we come to the equation that describes the dynamics of the vehicle along the tangent to its trajectory

$$\dot{v} = a(t) - c_0 v(t) - c_1 v(t)^2,$$

where $a(t) = F_x/m - c_r g$, $c_0 = k_{v0}/m$, $c_1 = k_{v1}/m$. In the previous equation, the lateral force contribution along the longitudinal dynamics was neglected being scaled by $\delta \approx 0$.

2.1.2 Acceleration Constraints

The vehicle dynamics is affected by different constraints on the available accelerations. A first *longitudinal constraint* comes from the limitations on the engine and braking power, i.e., $-\bar{a} \leq a(t) \leq \bar{a}$. The adherence between ground and tyre is modelled by the so called *friction ellipse*, which limits the feasible manoeuvres of the vehicle by constraining the lateral acceleration $a_l(t) = k(t)v^2(t)$ and the longitudinal acceleration $a(t)$ as follows:

$$\left(\frac{a(t)}{a_x}\right)^2 + \left(\frac{k(t)v^2(t)}{a_y}\right)^2 \leq 1, \quad (3)$$

where a_x and a_y are the maximum accelerations allowed for the longitudinal and lateral accelerations, respectively, and $k(t)$ is the curvature of the path. As in this paper we aim for semi-analytic solutions of the optimal control problem, the friction ellipse in (3) is too com-

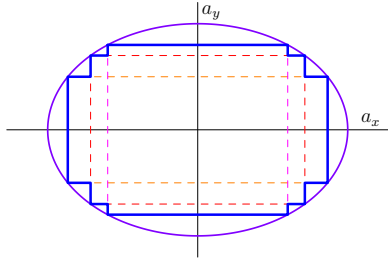


Figure 1. Various choices of the lateral acceleration constraints (dashed lines) and their envelope (thick line) inscribed in the friction ellipse.

plex to manage. Therefore, we will use a conservative approximation given by the combination of the longitudinal constraint $-\underline{a} \leq a(t) \leq \bar{a}$ with a lateral constraint of the form

$$|k(s)|v^2(s) \leq a_y. \quad (4)$$

This choice amounts to approximating the ellipse with an inscribed rectangle, as depicted in Figure 1.

2.2 Moving on Clothoid Arcs

As discussed above, by making the reasonable assumption that the steering angle is such that $\delta \approx \tan \delta$ and by restricting to control laws of the form of ω in (2), we can use the kinematic model (2), whose time-optimal solutions are clothoid arcs. We now offer a few numeric examples of how close a solution of this kind can be to the optimal solution.

The considered vehicle has the following parameters: $c_0 = 0.00002$, $c_1 = 0.0015$, the acceleration constraints considered in the example are $a_y = 5 \text{ m/s}^2$, $a \in [-5, 4] \text{ m/s}^2$. In a first scenario, we consider a lane change manoeuvre, in which the vehicle moves from initial position and velocity $(x_0, y_0) = (0, 0) \text{ m}$, $v_0 = 5 \text{ m/s}$, to final position $(x_f, y_f) = (50, 4) \text{ m}$, $v_f = 5 \text{ m/s}$. The optimal control Problem 1 is solved using both the kinematic model (1) and the transformed kinematic model (2), which produces a sequence of clothoids by definition. We also compute the clothoid joining the two points with assigned tangent using the geometric optimisation algorithm proposed in our previous work [5]. As shown in Figure 2.(a), the three curves are very difficult to distinguish in this case. Only by looking at the error plotted as a function of the curvilinear coordinate s denoting the progress along the curve, it is possible to appreciate the deviation between the two curves generated by the optimal solution of the dynamic problem for the two models from the clothoid identified by geometric considerations only. The maximum deviation is anyway quite small (below 5 cm over a total length of more than 50 m).

Depending on the length of the path and on the extremal points, we can have a more important deviation. This is

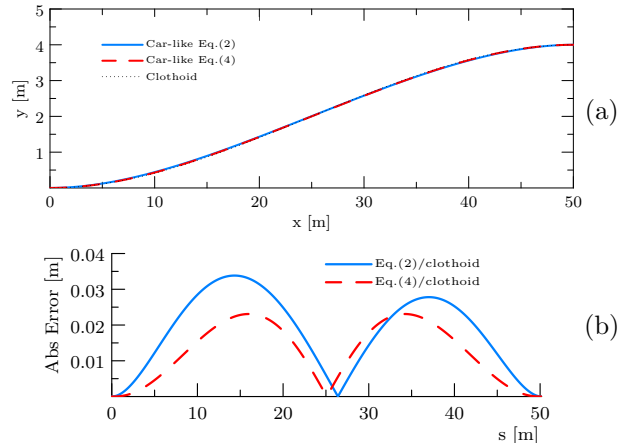


Figure 2. (a) Optimal trajectory of the unconstrained car-like model (1) (solid line), the trajectory of the deformed state space of Equation (2) (dashed line) and with the clothoid (dotted line) obtained from algorithm [5]. In (b) the absolute position error, which reaches a peak maximum of less than 4cm on a 50m manoeuvre.

shown in Figure 3. For this particular scenario, we considered an optimal solution for Problem 1 with the kinematic model (1) obtained with numeric methods. The optimal path was first compared with a single clothoid (dotted curve in Figure 3.(a)), found using the geometric optimisation tool [5] by imposing extremal points and tangent. In this case the deviation could well exceed 50 cm (see Figure 3.(b)), and have a significant impact on the travelled distance. In order to improve the result, we have broken the path in the middle and generated two clothoid segments. Once again, we have imposed in the tool the position and tangent at the extremal point and, for the middle point, we derived position and tangent from the optimal solution. The obtained curve is shown in dashed blue lines and the maximum deviation was reduced to below 25 cm. We have iterated the same procedure using two more intermediate points producing four clothoid segments. The reduction of the error was obviously more substantial (the maximum deviation is below 5 cm for a path longer than 100 m with a negligible impact of the approximation on the travelled distance. This example suggests that it is possible to obtain very close approximation of the optimal path using a sequence of clothoids, which can be possibly generated using a geometric optimisation tool. It could be argued that the shape of the optimal trajectory (and hence the quality of the approximation) is related to the maximum steering rate. The highest the value of the rate, the more the optimal trajectory is likely to deviate from a clothoid. Nevertheless, in our numeric examples we have used the maximum steering rate realistically achievable in automotive applications.

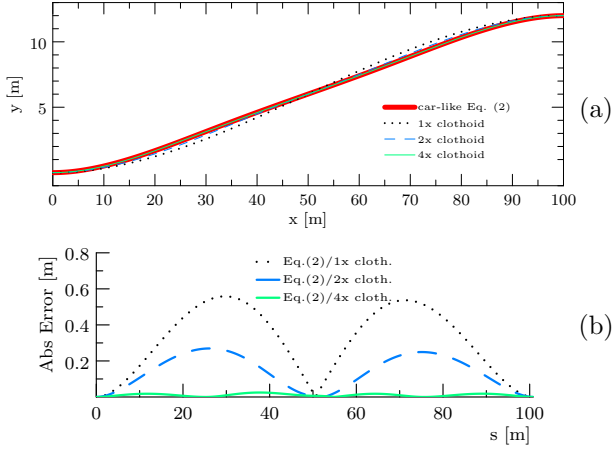


Figure 3. (a) Comparison on a long segment, the approximation of a 100m segment with one, two, and four equally spaced clothoids. In (b) the absolute error with respect to the original car-like model of Equation (1).

2.3 Modelling the Vehicle Motion on a Clothoid

Motivated by the discussion above, we will henceforth assume that the vehicle is constrained to move along a sequence of clothoids. Instrumental to the analysis in the following sections is rewriting the kinematic model under the assumption that the vehicle follows a clothoid.

Following a customary choice for path planning problems, this trajectory can be parametrised with the curvilinear abscissa $s(t)$, with a generic point of the trajectory being denoted as $(x_R(s), y_R(s))$. Let the initial and final point on the clothoid be $(x_R(0), y_R(0))$ and $(x_R(L), y_R(L))$ and the corresponding angles be ϑ_0 and ϑ_L . In order to uniquely specify the clothoid between the two given points, the length L and the two curvature parameters $\kappa_0, \kappa_1 \in \mathbb{R}$ are needed (see Figure 4). Indeed, the curvature of the clothoid is linear with the arc length and it is given by $k(s) = \kappa_0 + \kappa_1 s$, where the prime symbol is used to denote space derivation. Finding these parameters is equivalent to solving the G^1 Hermite interpolation problem, which requires to find κ_0, κ_1 and L of a clothoid that interpolates the assigned initial and final points and angles, producing a spline that has geometric continuity up to the first derivative (hence the name G^1) [5]. This clothoid of parametric equations (5) can be easily evaluated using the Fresnel generalised integrals [5] $X_k(a, b, c)$, $Y_k(a, b, c)$ for $s \in [0, L]$ as:

$$\begin{aligned} x_R(s) &= x_R(0) + sX_0(\kappa_1 s^2, \kappa_0 s, \vartheta_0), \\ y_R(s) &= y_R(0) + sY_0(\kappa_1 s^2, \kappa_0 s, \vartheta_0), \end{aligned} \quad (5)$$

where

$$\begin{aligned} X_n(a, b, c) &= \int_0^1 \tau^n \cos\left(\frac{a}{2}\tau^2 + b\tau + c\right) d\tau, \\ Y_n(a, b, c) &= \int_0^1 \tau^n \sin\left(\frac{a}{2}\tau^2 + b\tau + c\right) d\tau. \end{aligned}$$

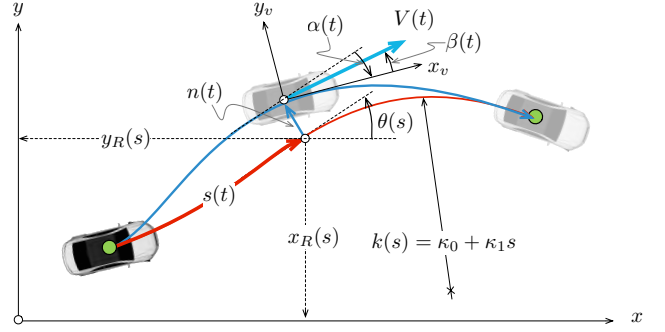


Figure 4. Curvilinear coordinates (s, n, α) defined with respect to a clothoid reference trajectory. X and Y represent the absolute frame axes, $V(t)$ is the absolute velocity of vehicle centre of mass, which is tangent to the trajectory, and $\beta(t)$ is the chassis slip angle. Finally, $\alpha(t)$ is the orientation of the vehicle w.r.t. reference line (i.e. clothoid) local tangent.

The derivative of the trajectory is usually expressed with trigonometric functions of the angle locally tangent to the reference trajectory $\theta(s)$,

$$\frac{d}{ds} x_R(s) = \cos \theta(s), \quad \frac{d}{ds} y_R(s) = \sin \theta(s).$$

It is worthwhile to note that for a clothoid the angle takes the form $\theta(s) = \frac{1}{2}\kappa_1 s^2 + \kappa_0 s + \vartheta_0$. The relation between θ and the curvature k is differential, i.e., $\theta'(s) = k(s) = \kappa_0 + \kappa_1 s$, that is, the clothoid has linear curvature.

The vehicle dynamics can be expressed in terms of its deviation from the reference trajectory. Let n denote the lateral displacement, i.e., n is the normal displacement of the vehicle with respect to the reference trajectory at the abscissa $s(t)$ (see Figure 4). Using the curvilinear coordinates representation, the absolute velocity of vehicle centre of mass $V(t)$ is tangent to the trajectory and, in general, it is not aligned with the vehicle X_v -axis forming an angle $\beta(t)$, named chassis slip angle. Additionally, the X_v -axis of the vehicle has an orientation $\alpha(t)$ with respect to the reference path (i.e., clothoid) local tangent. The vehicle kinematics can be given in terms of time and (x, y) coordinates defined as follows:

$$\begin{aligned} x(t) &= x_R(s(t)) - n(t) \sin \theta(s(t)), \\ y(t) &= y_R(s(t)) + n(t) \cos \theta(s(t)), \\ \psi(t) &= \alpha(t) + \theta(s(t)). \end{aligned} \quad (6)$$

Differentiating (6) with respect to the time variable t and substituting $\theta'(s) = k(s)$, yields:

$$\begin{aligned} \dot{x} &= x'_R \dot{s} - \dot{n} \sin \theta(s) - nk(s) \dot{s} \cos \theta(s), \\ \dot{y} &= y'_R \dot{s} + \dot{n} \cos \theta(s) - nk(s) \dot{s} \sin \theta(s), \\ \dot{\psi} &= \dot{\alpha} + k(s) \dot{s}. \end{aligned} \quad (7)$$

By combining the last equation of (6) with the model (2),

we have

$$\dot{x} = v \cos(\alpha + \theta), \quad \dot{y} = v \sin(\alpha + \theta),$$

that, substituted into (7) yields, after some algebra,

$$\dot{s} = v \cos \alpha / (1 - nk(s)), \quad \dot{n} = v \sin \alpha.$$

Moreover, by plugging the yaw rate relation of (7) in the model (2), we have

$$\dot{\alpha} = (v/l) \tan \delta - \dot{s}k(s).$$

Considering the dynamics of the longitudinal velocity, the complete model of the vehicle motion with respect to a single reference clothoid is finally given by

$$\begin{bmatrix} \dot{s} \\ \dot{n} \\ \dot{\alpha} \\ \dot{\delta} \\ \dot{v} \end{bmatrix} = \begin{bmatrix} v \cos \alpha / (1 - nk(s)) \\ v \sin \alpha \\ (v/l) \tan \delta - \dot{s}k(s) \\ \omega \\ a - c_0v - c_1v^2 \end{bmatrix}. \quad (8)$$

This model is in general hard or impossible to solve analytically. Indeed, while for specific classes of functions $a(t)$ a closed form solution can be found for the last equation describing the evolution of v (which has the form of a Riccati Differential Equation), this is obviously impractical for the remaining four non-linear and coupled ODEs. Therefore, we assume that: a) The vehicle is initially on the clothoid and with orientation aligned with the tangent of the clothoid ($n(0) = 0, \alpha(0) = 0$), b) The ideal controller

$$\omega = lk'(s)\dot{s}/(1 + l^2k(s)^2)$$

is assumed feasible and applied for $\dot{\delta}$ that enables a perfect tracking of the path (which is a common assumption [26]). Such assumptions guarantee that $n(t) = 0, \alpha(t) = 0, \forall t$, and from (6) that $\psi(t) = \theta(t)$. Thus the system of equations (8) simplifies to:

$$\dot{s} = v, \quad \dot{v} = a - c_0v - c_1v^2, \quad (9)$$

i.e., a system with the single input variable $a(t)$.

3 Solution for a Single Clothoid

By accounting for the constraint that the vehicle moves according to model (9), Problem 1 can be written as follows.

Problem 2 Find control $a(t)$ that minimises the total time T subject to:

$$\text{ODE : } \begin{cases} \dot{s}(t) = v(t), \\ \dot{v}(t) = a(t) - c_0v(t) - c_1v^2(t), \end{cases}$$

$$\text{Boundary Conditions } \begin{cases} v(0) = v_0, & s(0) = 0, \\ v(T) = v_f, & s(T) = L, \end{cases}$$

$$\text{Constraints } \begin{cases} -\underline{a} \leq a(t) \leq \bar{a}, \\ |k(s(t))|v(t)^2 \leq a_y. \end{cases}$$

Since the bound on the lateral acceleration of the OCP is a function of the state only (and not of the control variable), we can solve the problem in two phases. In the first phase, we solve the OCP accounting only for the longitudinal constraint. In the second, we consider also the lateral constraint. For the first problem, the Hamiltonian of the minimum time Problem 2 is

$$\mathcal{H} = 1 + \lambda_1(a - c_0v - c_1v^2) + \lambda_2v,$$

where 1 is the Lagrange term representing minimum time and λ_i are the Lagrangian multipliers of the corresponding differential equations, for v and s respectively [2]. Since the control $a(t)$ appears linearly, its optimal synthesis is obtained from Pontryagin's Maximum Principle (PMP), and is given by

$$a(t) = \arg \min \mathcal{H} = \begin{cases} \bar{a} & \text{if } \lambda_1 < 0, \\ -\underline{a} & \text{if } \lambda_1 > 0, \\ a_{\text{sing}} & \text{if } \lambda_1 \equiv 0. \end{cases}$$

The control $a(t)$ is bounded in the interval $[-\underline{a}, \bar{a}]$, hence the solution of the PMP produces a typical *bang-bang controller*. The term a_{sing} represents a possible singular control when λ_1 is identically zero on an interval, however, in our specific case, singular controls are not present in the solution, as discussed in [2] Ch. 7.11.

According to a well known result in Optimal Control Theory (e.g. [2] Ch. 7.11), if the Problem 2 solution without constraints exists, it has at most one control switching time instant t_s . This implies that the optimal control has to be chosen from a family of four candidate controls. The first and second correspond to pure acceleration (i.e., the $a(t) \equiv \bar{a}$) or braking manoeuvre (i.e., $a(t) \equiv -\underline{a}$), the third and fourth are a combination of the two. Having explicit expressions for the optimal states, with the complete boundary conditions, the solution of each case is obtained by the solution of a nonlinear system in two unknowns: the switching time t_s and the final time T . It is possible to rule out the case of a braking manoeuvre followed by an acceleration because it is not time optimal. We can consider only the case of acceleration and braking with a switching time and recover the case of pure acceleration or pure braking as degenerate cases when the switching time takes 0 or the final time T . It follows that the solution is given by the intersection at the switching point t_s of the two curves of the velocity $v(t)$ and the space $s(t)$. Having an explicit analytic solution of the state variables allows us to quickly find the intersection point.

3.1 Analytic Solutions of the Dynamic System

The analytic integration of the dynamic system in Problem 2 is crucial for the solution. There are combinations of the parameters c_0 and c_1 , as well as critical boundary values, that change the shape of the solution. Moreover, even if expressed by elementary functions, the analytic

solutions are numerically unstable. A numerically stable solution is contained in the following lemmas. A complete discussion and the proof is deferred to a technical report [6] for space reasons. The lemmas contain analytic expressions for $v(t)$ and $s(t)$, and are based on the following auxiliary constants:

$$\begin{aligned} w &\triangleq \sqrt{c_0^2 + 4ac_1}, \quad \alpha \triangleq \frac{w + c_0}{2}, \quad \beta \triangleq \frac{w - c_0}{2}, \\ \gamma &\triangleq c_1 v_\star + \alpha, \quad v_\infty \triangleq \frac{\beta}{c_1} = \frac{a}{\alpha}, \quad a_0 \triangleq (c_1 v_\star + c_0) v_\star. \end{aligned} \quad (10)$$

Notice that according to the values of c_0 , c_1 and $a(t)$, the value w can be real (without loss of generality assumed positive) or complex. The *asymptotic speed* v_∞ is the speed asymptotically reached by the vehicle starting from rest and moving straight with maximum acceleration.

Lemma 3 *Let $v(t; v_\star)$ be the analytic solution of (9) with initial velocity v_\star . For $w \geq 0$ or equivalently $c_0^2 + 4ac_1 \geq 0$, the solution takes the following forms*

$$v(t; v_\star) = v_\star + \frac{(a_0 - a) \mathcal{E}(t, w)}{1 - \gamma \mathcal{E}(t, w)},$$

where $\mathcal{E}(t, w) \triangleq (1 - e^{wt})/w$ and where the constants are defined in (10). If w is imaginary, the velocity takes the form

$$v(t; v_\star) = \frac{\sin(\theta_0 - \frac{1}{2}t|w|) \sqrt{|a|}}{\sin(\theta_1 + \frac{1}{2}t|w|) \sqrt{c_1}},$$

where

$$\begin{aligned} \theta &= \arctan(|w|/c_0), \\ \theta_0 &= \arctan((v_\star |w|)/(v_\star c_0 + 2|a|)), \\ \theta_1 &= \theta - \theta_0 = \arctan(|w|/(2c_1 v_\star + c_0)). \end{aligned} \quad (11)$$

The solution $v(t; v_\star)$ is meaningful only for finite non-negative values.

The space variable s has the analytic expression given in the next lemma.

Lemma 4 *Let $s(t; v_\star) = \int_0^t v(\zeta; v_\star) d\zeta$ be the space swept with the velocity $v(t; v_\star)$, then*

$$s(t; v_\star) = \begin{cases} v_\infty t + c_1^{-1} \log(1 - c_1(v_\infty - v_\star) \mathcal{E}(-t, w)), \\ c_1^{-1} \left(\log\left(\frac{\sin(\theta_1 + \frac{1}{2}t|w|)}{\sin \theta_1}\right) - \frac{c_0}{2}t \right), \end{cases}$$

where the first is valid for w real and the second for w imaginary. The value of θ_0 and θ_1 are defined in equation (11).

3.2 Switching Time and Minimum Time Computation

Having explicit expressions for $v(t)$ and $s(t)$, the first step towards the solution of the OCP 2 is to find the

bang-bang solution of the problem without lateral acceleration constraint. This amounts to finding the optimal switching instant t_s and the final minimum time T , which is done equating the arcs of positive acceleration of velocity and space with the corresponding arcs of negative acceleration. The result is the following system of two nonlinear equations in the unknowns t_s and T :

$$\begin{aligned} v(t_s; v_0, \bar{a}) &= v(t_s - T; v_f, \underline{a}), \\ s(t_s; v_0, \bar{a}) &= s(t_s - T; v_f, \underline{a}) + L. \end{aligned} \quad (12)$$

In these expressions, we have exposed the dependence on the control $a(t)$ in order to distinguish the arcs of acceleration and deceleration and to avoid ambiguities. It is possible to analytically solve the first equation in (12) with respect to T and to substitute the value in the second equation. This would yield a single nonlinear equation, however it is better to solve the 2×2 nonlinear system, because of the higher computational cost of the inverse of $v(t)$ with respect to T and its derivative in a Newton method. Let a_L, a_R, v_L, v_R, s_L and s_R be the following short-cut quantities:

$$\begin{aligned} s_L &\triangleq s(t_s; v_i, \bar{a}), & s_R &\triangleq s(t_s - T; v_f, \underline{a}) \\ v_L &\triangleq v(t_s; v_i, \bar{a}), & v_R &\triangleq v(t_s - T; v_f, \underline{a}) \\ a_L &\triangleq \bar{a} - c_0 v_L - c_1 v_L^2, & a_R &\triangleq -\underline{a} - c_0 v_R - c_1 v_R^2, \end{aligned}$$

we finally have the following vector valued map $F: \mathbb{R}^2 \mapsto \mathbb{R}^2$ that we use to model and solve the nonlinear system (12). Both the function $F(t_s, T)$ and its Jacobian J are employed in the numeric method. The Jacobian of the system can be analytically constructed and symbolically inverted once we compute the derivatives of $s(t)$ and $v(t)$, which are readily obtained by the ODEs. The explicit form of F and of J is given by:

$$F(t_s, T) = \begin{pmatrix} v_L - v_R \\ s_L - s_R - L \end{pmatrix}, \quad J = \begin{pmatrix} a_L - a_R & a_R \\ v_L - v_R & v_R \end{pmatrix}.$$

The use of a robust nonlinear solver, e.g., a Levenberg-Marquardt method or any other approach based on trust-regions, produces a fast algorithm that converges in 4-5 iterations. This step produces t_s and T which are the solutions of the switching time and the optimal time for the bang-bang problem.

3.3 The Bound on the Lateral Acceleration

The next step is to introduce the constraint (4) on the lateral acceleration. When this bound is considered, the *a priori* knowledge of the curvature and the length of the clothoid travelled by the vehicle is conveniently used. When the constraint is active, the evolution of the system has to respect the equation $|k(s)|v(s)^2 = a_y$. Hence, we have to translate this relation into an analytic expression for $a(t)$, $v(t)$ and $s(t)$. The control $a(t)$ appears only implicitly in the bound. In order to determine its value, it is necessary to differentiate it and substitute

the corresponding value of the differential equations (9) for the state variable $v(t)$. This can be done using either time or space as independent variable. It is preferable to use space because the resulting expressions are easier to manipulate. The differential equation for the velocity, parametrised with the space $s(t)$ is, after the corresponding change of variable, given by

$$v'(s) = \frac{a(s)}{v(s)} - c_0 - c_1 v(s). \quad (13)$$

The derivative of the bound gives

$$\text{sign}(k(s)) \kappa_1 v^2(s) + |k(s)| v'(s) v(s) = 0,$$

and we substitute $v'(s)$ with the ODE (13) obtaining

$$\kappa_1 v^2(s) \text{sign } k(s) + |k(s)| (a(s) - c_0 v(s) - c_1 v^2(s)) = 0.$$

Substituting the equation of the bound for $v(s)$ gives an explicit solution for the control $a(s)$ (the constraint has order 1) when the lateral acceleration constraint is active (henceforth defined “constrained arc acceleration”):

$$a(s) = c_0 \sqrt{\frac{a_y}{|k(s)|}} + \frac{a_y c_1}{|k(s)|} - \frac{\kappa_1 a_y \text{sign } k(s)}{2 |k(s)|^2}, \quad (14)$$

with the velocity given by the bound

$$v(s) = \sqrt{a_y / |k(s)|}. \quad (15)$$

The analytic expression above is obviously more efficient to compute than any numeric algorithm of our knowledge. The denominator in the previous expression is different from zero if the curvature is different from zero, but when the curvature is zero, the bound cannot be active by definition (i.e., the condition of the constraint becomes $0 \leq a_y$), hence the constrained arc control in this case is well defined, i.e., the vehicle is travelling on a straight path. The restriction to clothoids introduces a remarkable simplification because the zero curvature points are easily identified (being $k(s)$ a linear function). This is not generally true for different motion primitives (e.g., cubic or quintic splines), for which our approach is only applicable as a numeric procedure.

3.4 Construction of the Optimal Solution

The optimal acceleration profile solving the OCP 2 can be constructed by intersecting the analytic expression for the bang-bang solution contained in Equation (12) with the velocity when lateral bound is active contained in Equations (14), (15). This simple curve intersection problem can be solved numerically and used to produce the optimal control. A possible algorithm to do this is discussed in our previous work [19]. In the next section, we will solve the problem in a more general case (sequence of clothoids).

4 Optimal Solution for a Sequence of Clothoids

In the previous section, we have provided all the elements that are needed to compute the optimal acceleration profile when the vehicle is constrained to move on a clothoid segment. We now show an algorithm, called Forward-Backward Algorithm, that uses these elements to find the OCP solution for a trajectory comprising a sequence of connected clothoids, which we will refer to as *path*. This is a remarkable achievement of this paper since it allows to compute the optimal control for generic paths, such as road sectors, intersections or racetracks. The algorithm is described in the following five steps. In the algorithm description we will use as a running example the path shown in Figure 5, whose curvature is displayed in the uppermost plot of Figure 6. In the example there is a discontinuity in the curvature, which we have included to point out the absence on any continuity assumption.

(1) **Preprocessing.** During this step, we identify the segments in which the lateral constraint can become active and the segments with longitudinal constraints only. To achieve this goal, we first identify the segments where the curvature has constant sign. For these segments, we compute the maximum velocity using Equation (15). In order to simplify the algorithm formulation, it is useful to introduce a maximum velocity v_{\max} , which is generally greater than the asymptotic speed v_{∞} . This value is used to clip the maximum velocity resulting from the lateral bound. If the lateral bound is active and less than v_{\max} on the whole segment, we classify the segment as **saturated**; if the lateral bound is never active or v_{\max} is less than the saturated velocity the classification is **clipped**; otherwise we split the segment into two other segments, one **saturated** and one **clipped**. At the end of this phase there are only **clipped** or **saturated** segments. The result of this step on the example is shown in the second plot of Figure 6, where $v_{\max} = 80$ m/s, the horizontal blue lines are the **clipped** segments and the orange arcs are the **saturated** segments. In all the **clipped** segments we will have a bang-bang arc (i.e., extremal values for the acceleration) in the final solution. For the **saturated** parts, we will eventually use the singular acceleration in Equation (14) only if it meets all the other constraints, e.g., it could be that staying on the lateral constraint requires an unfeasible value for the acceleration.

(2) **Saturation Analysis.** After the preprocessing step, there can be arcs where the lateral bound is active that do not satisfy the constraint on the longitudinal acceleration, i.e., considering $a \in [-\underline{a}, \bar{a}]$ the corresponding velocity cannot be achieved for physical limitation on the actuators or for the action of friction and aerodynamic drag. To obtain only admissible arcs, we then cut the singular control in $[-\underline{a}, \bar{a}]$. This requires to solve Equation (14) that represents a quartic polynomial (more details on this in Remark 2). The result is shown in the third

plot of Figure 6. After this phase, we have identified all the segments (orange arcs) that can possibly have the lateral constraint active in the final solution because the required acceleration respects both the lateral and the longitudinal constraints.

(3) **Forward Sweep.** Starting from the first segment, integrate forwards in space (exploiting the analytic solution) and sequentially the velocity with the maximum acceleration allowed. With a slight abuse of notation, we will denote by v_R the initial velocity for each segment. For the first segment, v_R is either set to v_{\max} or set to the saturated value (if the bound is active). For any other segment v_R is set to the final velocity of the previous segment in the sequence. For each segment, we compute the velocity profile at maximum acceleration starting from v_R . If the resulting velocity profile is below the profile computed at the previous step, the segment is classified as **push** and the new profile substitutes the previous one. If the new velocity profile is above the previous one the segment is left unchanged in order not to violate the lateral constraint. If the profile intersects the segment, it is split at the intersection and the first part is classified as **push**. At the end of this phase there are only **push**, **saturated** and **clipped** segments (green, orange and blue lines of the fourth plot of Figure 6, respectively). In the same figure, we observe that in the first **push** segment the velocity decreases despite the maximum acceleration is used. This is an effect of the aerodynamic drag because the initial speed provisionally chosen (80m/s) is greater than v_∞ .

(4) **Backward Sweep.** To remove the discontinuity in the velocity profile, we analyse the profiles backwards from the last to the first. For a given segment, let v_L denote the velocity at the beginning of the segment and v_R the velocity at end of the previous one. If they are equal, we accept the segment, otherwise it must be $v_R > v_L$ (by construction $v_R < v_L$ is not possible) and we have to compute a maximum braking manoeuvre ($a = -\underline{a}$) and check for an intersection inside the previous segment: if there exists such an intersection, we modify the segment classification right after the intersection point with **brake**; if the intersection is not in the previous segment, we reclassify the whole segment as **brake**. At the end of this phase there are only three types of segment: **brake**, **push** and **saturated** (red, green and orange segments of the fifth plot of Figure 6, respectively). The obtained velocity profile is the maximum possible speed profile for the path. The associated travelling time is the minimum time that it is possible to obtain, i.e. we have identified the maximum initial velocity and the maximum final velocity at the extreme of the path.

(5) **Matching of the Boundary Conditions.** Having the maximum velocities at the boundaries of the path, it is easy to determine if the OCP problem has a solution or not. If the boundary velocities are greater than the maximum allowed velocities, there is no solution, otherwise

the solution is obtained by intersecting the integration of the velocity obtained with maximum $a = \bar{a}$ (first segment) or minimum $a = -\underline{a}$ (last segment) accelerations with the previous velocity profile (see the sixth plot of Figure 6). The corresponding optimal control is synthesised from the classification of the segments of this last phase, for **push** segments $a = \bar{a}$, for **brake** segments it is set to $a = -\underline{a}$ and for **saturated** segments is given by (14) (lowermost plot of Figure 6).

The trajectory obtained with the Forward-Backward Algorithm is optimal as shown in the following.

Theorem 5 *The result given by the Forward-Backward Algorithm of Section 4 gives the global minimum time trajectory of Problem 2.*

PROOF. The proof is given by contradiction. First we consider that there are no singular arcs in the optimal solution of the unconstrained problem, as shown in Section 3 (see also [2]), then by the results of [27], extended by [10], the junction points with the constraint are not essential touch points, but proper intervals (because the constraint has order 1). Moreover we notice that the constraint in each segment after the preprocessing step is monotone (see Figure 6, second plot), a fact that simplifies the discussion of the intersections. The time optimal problem is equivalent to the problem of maximising the velocity over the considered interval, because $\min T = \min \int_0^L 1/v ds$.

If there exists a trajectory γ' that yields a lower optimal time manoeuvre, then for the continuity of the velocity profile v , there must be a point (s^*, v^*) (and thus a whole interval around that point) where the velocity of this new trajectory is higher than the velocity of the trajectory γ given by the algorithm. This point cannot be located in arcs where the algorithm gives constrained arcs, because there the velocity is the maximum feasible and is given by the constraint itself. Hence (s^*, v^*) must lie where γ is unconstrained, e.g. bang-bang. The trajectory γ' in (s^*, v^*) can be extended forward and backward and must intersect the trajectory γ in at least two points, otherwise it would either not match the boundary conditions or leave the admissible region. These two points are located at the left and at the right of (s^*, v^*) . Because of optimality, the arcs of maximum acceleration precede the arcs of maximum deceleration, γ' must intersect γ either at the acceleration arc twice, at the deceleration arc twice or once at the acceleration and once at the deceleration. But since the control in γ was chosen on the boundary of $[-\underline{a}, \bar{a}]$ those cases lead to a contradiction, thus γ is the global optimal trajectory. \square

Remark 1 *For curves different from clothoids, this algorithm loses its simplicity and effectiveness, so more sophisticated algorithms must be used [42,41]. Nevertheless, those algorithms are computationally heavy, mainly*

because of the backtracking process for curvatures that are no more linear. What makes the present algorithm particularly effective for clothoids is the possibility of a light backtracking process (one forward and one backward sweep), the fast computation of the closed form analytic solutions of the dynamic system and the necessity of numeric computation only for the switching points.

Remark 2 The most complicated part of the algorithm is finding the switching points between a regular and a singular arc. In particular, attention must be paid in these transitions. To efficiently tackle this problem, it is therefore mandatory to analyse the singular arcs and to cut them into the admissible interval $[-\underline{a}, \bar{a}]$. More precisely, the equation (14) has to be equated to $-\underline{a}$ and \bar{a} and solved properly. In order to solve this numerically challenging equation involving a quartic polynomial, we implemented a solver based on the work of [17].

5 Numerical Results

A sketch of the clothoids used for the running example of Figure 6 represented in the (x, y) plane is reported in Figure 5. The comparison between the numerical solutions and the OCP solution is also reported. The data describing the example are the following: the curvature at the corner points is (as vector - notice that the curvature is not continuous but only piecewise continuous, a weaker condition) $\kappa_0 = [0, 0, 0.008, 0.008, -0.002, 0.01, 0.01, -0.00242, -0.00342, 0.00458]$, the vector of the lengths is $s = [0, 150, 300, 600, 800, 800, 1000, 1000, 1100, 1300]$. The nodes in s are duplicated when there is a jump in the curvature, otherwise the curvature is a continuous function at each node, see the first plot of Figure 6. The boundary conditions are given as an initial velocity of 25 m/s and a final velocity of 15 m/s. The parameters of the vehicle are $c_0 = 0.00002$, $c_1 = 0.0015$, $a_y = 5 \text{ m/s}^2$, $a \in [-5, 4] \text{ m/s}^2$ with $v_{\max} = 80 \text{ m/s}$. The optimal time computed with the present algorithm is 41.1828 seconds, the execution time was 1 millisecond on the Matlab implementation and 0.12 milliseconds on the C++ version, that is approximately 0.02 milliseconds per clothoid segment.

On the other hand on a C++ Optimal Control Solver like Pins [7], which are state of the art for these problems, the execution time is around 1 second on the same example and same machine (a Mac Book Pro with Intel Core i7 2.6 GHz). We tested the algorithm also for longer sequences of clothoids, up to 100.000 consecutive segments (a total length of 1000 km), and the running time was around 270 milliseconds (in C++), while it was 2.7 seconds for one million of segments (a total length of 10000 km), from which we argue that the algorithm has linear complexity with respect to the number of segments. These examples cannot be treated by the numeric solvers because of the large amount of resulting equations. We tested

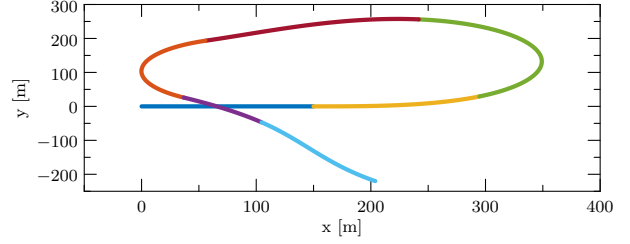


Figure 5. The trajectory of the clothoid sequence of the running example proposed in Section 5.

the algorithm also on an embedded platform (a beaglebone¹, endowed with a 720 MHz Cortex-A8 processor), the computational time is around ten times slower with respect to the i7 machine. The results obtained with the OCP numeric solvers like Pins and Gpops-II [35] give a slightly higher target time, mainly due to the numeric approximations. However, very different are the computational costs in terms of execution time. A direct comparison is not possible, because of the different implementations and approach, moreover the execution time of these numerical methods varies also on the basis of the initial guess and on the mesh grid adopted. In the best case, we were able to run a simulation in around 1.6 seconds with a target of 41.1946 seconds, in the worst case, when we required higher accuracy and smaller tolerances, the execution time grew up to 25 seconds.

6 Conclusions and Future Developments

We have shown a solution for the computation of a minimum time manoeuvre for a car-like vehicle subject to longitudinal and lateral acceleration constraints and moving along a clothoid segment. This solution consists of arcs run at maximum acceleration, minimum acceleration and at the maximum acceleration compatible with the constraints, for which we give an analytical expression. The switching instants are computed by solving simple polynomial equations. We also proposed an algorithm that uses these solution to construct the optimal manoeuvre for a sequence of clothoids. It is worthwhile to note that the semi-analytic solution to the optimal control problem with “rectangular” constraints on the acceleration (see Figure 1) can be readily used to solve the problem for the actual ellipsoid constraint of a_y . Indeed, by approximating the ellipsoid as the envelope of an arbitrary number of rectangles, it is possible to combine the obtained optimal solutions and thus have an actual sub-optimal solution with the desired level of accuracy.

Several points remain open that will stimulate future research activities. We just name a few. First, the linear curvature of the clothoids gives evident advantages

¹ <http://beagleboard.org/bone>

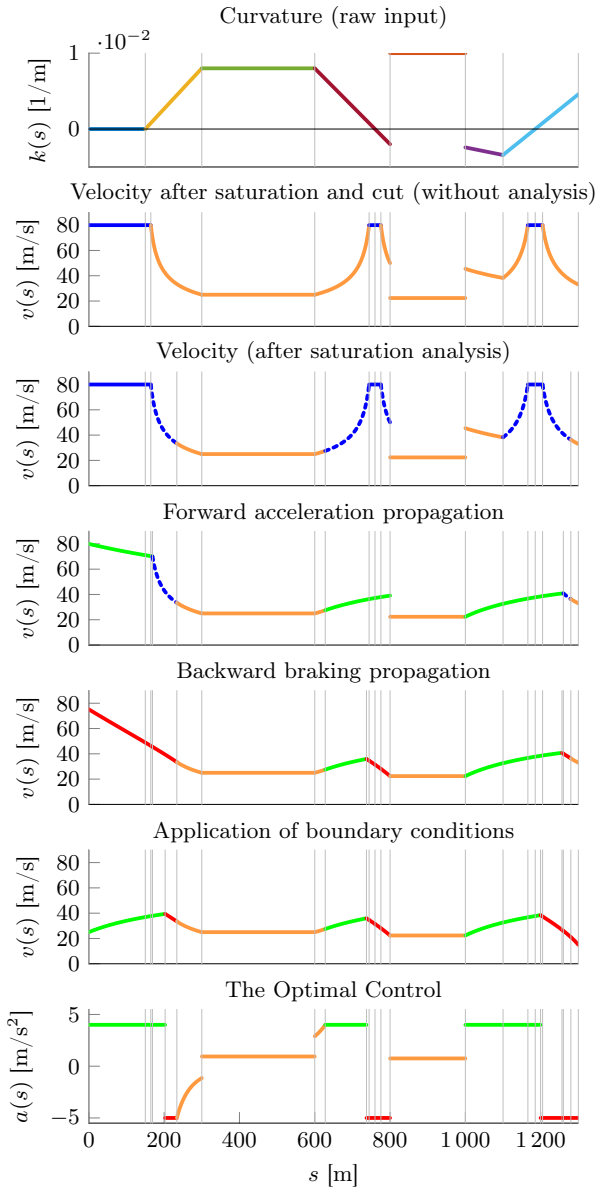


Figure 6. From the top: 1) the user supplied curvature profile of the path; 2) the velocity on the generated segments, blue dashes are **clipped** segments, orange the **saturated**; 3) the second step of analysis, where the control limitations in $[-\bar{a}, \bar{a}]$ are taken into account; 4) the result of the velocity of the forward sweep, there are **clipped**, **push** and **saturated** intervals (resp. blue dashed, green and orange); 5) the backward sweep, with the introduction of the **brake** intervals in red (at the end of this phase the result is the maximum speed profile of the clothoid sequence); 6) the connection with the boundary conditions that gives the desired speed profile and the segments are classified as **push** (green), **brake** (red) and **saturated** (orange); 7) the optimal control, synthesised from this classification.

in our framework. How much of the efficiency of our solution can be retained for different curves remains to be seen. Another research direction is how to set up a

proper exchange of information between geometric exploration (the master problem) and manoeuvre optimisation (the slave problem, presented in this paper), in order to ensure a first convergence of the former to a good sub-optimal solution. This is particularly useful if the planning algorithm is to be implemented on a vehicle and executed in real-time on an embedded architecture. A third item in our working agenda is how to use our results in a game-theoretic framework, in which different vehicles compete to overtake each other.

References

- [1] E. P. Anderson, R. W. Beard, and T. W. McLain. Real-time dynamic trajectory smoothing for unmanned air vehicles. *IEEE Transactions on Control Systems Technology*, 13(3):471–477, May 2005.
- [2] M. Athans and P.L. Falb. *Optimal Control: An Introduction to the Theory and Its Applications*. Lincoln Laboratory publications. McGraw-Hill, 1966.
- [3] J. Barraquand, B. Langlois, and J-C. Latombe. Numerical potential field techniques for robot path planning. *Systems, Man and Cybernetics, IEEE Transactions on*, 22(2):224–241, 1992.
- [4] E. Bertolazzi, F. Biral, M. Da Lio, A. Saroldi, and F. Tango. Supporting drivers in keeping safe speed and safe distance: The SASPENICE subproject within the european framework programme 6 integrating project prevent. *IEEE Transactions on Intelligent Transportation Systems*, 11(3):525–538, 2010.
- [5] E. Bertolazzi and M. Frego. G^1 fitting with clothoids. *Mathematical Methods in the Applied Sciences*, 38(5):881–897, 2015.
- [6] E. Bertolazzi and M. Frego. Semi-Analytical Minimum Time Solution for the Optimal Control of a Vehicle subject to Limited Acceleration. *Optimal Control, Applications and Methods*, submitted.
- [7] F. Biral, E. Bertolazzi, and P. Bosetti. Notes on numerical methods for solving optimal control problems. *IEEJ Journal of Industry Applications*, 5(2):154–166, 2016.
- [8] F. Biral, E. Bertolazzi, and M. Da Lio. *Modelling, Simulation and Control of Two-Wheeled Vehicles*, chapter The Optimal Manoeuvre, pages 119–154. John Wiley & Sons, Ltd, 2014.
- [9] F. Biral, R. Lot, S. Rota, M. Fontana, and V. Huth. Intersection support system for powered two-wheeled vehicles: Threat assessment based on a receding horizon approach. *IEEE Transactions on Intelligent Transportation Systems*, 13(2):805–816, 2012.
- [10] J.F. Bonnans and A. Hermant. Second-order analysis for optimal control problems with pure state constraints and mixed control-state constraints. *Annales de l’Institut Henri Poincaré (C) Non Linear Analysis*, 26(2):561 – 598, 2009.
- [11] P. Bosetti, M. Da Lio, and A. Saroldi. On the human control of vehicles: an experimental study of acceleration. *European Transport Research Review*, 6(2):157–170, 2014.
- [12] A. Broggi, M. Buzzoni, S. Debattisti, P. Grisleri, M.C. Laghi, P. Medici, and P. Versari. Extensive tests of autonomous driving technologies. *Intelligent Transportation Systems, IEEE Transactions on*, 14(3):1403–1415, 2013.
- [13] W-w. Cai, L-p. Yang, and Y-w. Zhu. Bang-bang optimal control for differentially flat systems using mapped pseudospectral method and analytic homotopic approach.

- Optimal Control Applications and Methods*, 37(6):1217–1235, 2016.
- [14] M. Da Lio, F. Biral, E. Bertolazzi, M. Galvani, P. Bosetti, D. Windridge, A. Saroldi, and F. Tango. Artificial co-drivers as a universal enabling technology for future intelligent vehicles and transportation systems. *Intelligent Transportation Systems, IEEE Transactions on*, 16(1):244–263, Feb 2015.
- [15] D. Dolgov, S. Thrun, M. Montemerlo, and J. Diebel. Path planning for autonomous vehicles in unknown semi-structured environments. *The International Journal of Robotics Research*, 29(5):485–501, 2010.
- [16] L. E. Dubins. On curves of minimal length with a constraint on average curvature, and with prescribed initial and terminal positions and tangents. *American Journal of mathematics*, pages 497–516, 1957.
- [17] N. Flocke. Algorithm 954: An accurate and efficient cubic and quartic equation solver for physical applications. *ACM Trans. Math. Softw.*, 41(4):30:1–30:24, October 2015.
- [18] T. Fraichard and A. Scheuer. From reeds and shepp’s to continuous-curvature paths. *Robotics, IEEE Transactions on*, 20(6):1025–1035, Dec 2004.
- [19] M. Frego, E. Bertolazzi, F. Biral, D. Fontanelli, and L. Palopoli. Semi-analytical minimum time solutions for a vehicle following clothoid-based trajectory subject to velocity constraints. In *2016 European Control Conference (ECC)*, pages 2221–2227, June 2016.
- [20] M. Frego, P. Bevilacqua, E. Bertolazzi, F. Biral, D. Fontanelli, and L. Palopoli. Trajectory Planning for Car-like Vehicles: a Modular Approach. In *Proc. IEEE Int. Conf. on Decision and Control (CDC)*, pages 203–209, Las Vegas, Nevada, US, Dec. 2016. IEEE.
- [21] N.A. Greenblatt. Self-driving cars and the law. *IEEE Spectrum*, 53(2):46–51, 2016.
- [22] M. Guiggiani. *The Science of Vehicle Dynamics: Handling, Braking, and Ride of Road and Race Cars*. SpringerLink : Bücher. Springer Netherlands, 2014.
- [23] E. Guizzo. How google’s self-driving car works. *IEEE Spectrum Online*, October, 18, 2011.
- [24] J. Hauser and A. Saccon. Motorcycle modeling for high-performance maneuvering. *IEEE Control Systems*, 26(5):89–105, Oct 2006.
- [25] S. Hota and D. Ghose. Optimal transition trajectory for waypoint following. In *2013 IEEE International Conference on Control Applications (CCA)*, pages 1030–1035, Aug 2013.
- [26] G. Indiveri and M.L. Corradini. Switching linear path following for bounded curvature car-like vehicles. In *Proceedings of the IFAC Symposium on Intelligent Autonomous Vehicles*, 2004.
- [27] D.H Jacobson, M.M Lele, and J.L Speyer. New necessary conditions of optimality for control problems with state-variable inequality constraints. *Journal of Mathematical Analysis and Applications*, 35(2):255–284, 1971.
- [28] S. Karaman and E. Frazzoli. Sampling-based algorithms for optimal motion planning. *The International Journal of Robotics Research*, 30(7):846–894, 2011.
- [29] S. Karaman, M.R. Walter, A. Perez, E. Frazzoli, and S. Teller. Anytime motion planning using the RRT*. In *Robotics and Automation (ICRA), 2011 IEEE International Conference on*, pages 1478–1483. IEEE, 2011.
- [30] J.J. Kuffner and S.M. LaValle. RRT-connect: An efficient approach to single-query path planning. In *Robotics and Automation, 2000. Proceedings. ICRA’00. IEEE International Conference on*, volume 2, pages 995–1001. IEEE, 2000.
- [31] Y. Kuwata, S. Karaman, J. Teo, E. Frazzoli, J.P. How, and G. Fiore. Real-time motion planning with applications to autonomous urban driving. *Control Systems Technology, IEEE Transactions on*, 17(5):1105–1118, Sept 2009.
- [32] R. Lot and N. Dal Bianco. Lap time optimisation of a racing go-kart. *Vehicle System Dynamics*, 54(2):210–230, 2016.
- [33] D. Mellinger and V. Kumar. Minimum snap trajectory generation and control for quadrotors. In *2011 IEEE International Conference on Robotics and Automation*, pages 2520–2525, May 2011.
- [34] W.F. Milliken and D.L. Milliken. *Race Car Vehicle Dynamics*. Premiere Series. Society of Automotive Engineers, 1995.
- [35] M.A. Patterson and A.V. Rao. GPOPS-II: A MATLAB software for solving multiple-phase optimal control problems using hp-adaptive gaussian quadrature collocation methods and sparse nonlinear programming. *ACM Trans. Math. Softw.*, 41(1):1–37, October 2014.
- [36] G. Perantoni and D.J.N. Limebeer. Optimal control for a formula one car with variable parameters. *Vehicle System Dynamics*, 52(5):653–678, 2014.
- [37] Y-Q. Qin, D-B. Sun, N. Li, and Y-G. Cen. Path planning for mobile robot using the particle swarm optimization with mutation operator. In *Machine Learning and Cybernetics, 2004. Proceedings of 2004 International Conference on*, volume 4, pages 2473–2478. IEEE, 2004.
- [38] C. Richter, A. Bry, and N. Roy. *Polynomial Trajectory Planning for Aggressive Quadrotor Flight in Dense Indoor Environments*, pages 649–666. Springer International Publishing, 2016.
- [39] T. Rizano, D. Fontanelli, L. Palopoli, L. Pallottino, and P. Salaris. Global path planning for competitive robotic cars. In *Decision and Control (CDC), 2013 IEEE 52nd Annual Conference on*, pages 4510–4516. IEEE, 2013.
- [40] R.G. Sanfelice, S.Z. Yong, and E. Frazzoli. On minimum-time paths of bounded curvature with position-dependent constraints. *Automatica*, 50(2):537–546, 2014.
- [41] Z. Shiller and H.-H. Lu. Robust computation of path constrained time optimal motions. In *Robotics and Automation, 1990. Proceedings., 1990 IEEE International Conference on*, pages 144–149 vol.1, May 1990.
- [42] K.G. Shin and Neil D. McKay. Minimum-time control of robotic manipulators with geometric path constraints. *Automatic Control, IEEE Transactions on*, 30(6):531–541, 1985.
- [43] D. Tavernini, M. Massaro, E. Velenis, D.I. Katzourakis, and R. Lot. Minimum time cornering: the effect of road surface and car transmission layout. *Vehicle System Dynamics*, 51(10):1533–1547, 2013.
- [44] C. Urmson et al. Autonomous driving in urban environments: Boss and the urban challenge. *Journal of Field Robotics*, 25(8):425–466, 2008.
- [45] E. Velenis and P. Tsiotras. Minimum-time travel for a vehicle with acceleration limits: Theoretical analysis and receding-horizon implementation. *Journal of Optimization Theory and Applications*, 138(2):275–296, 2008.